

Current Biology

The rise of pelagic sharks and adaptive evolution of pectoral fin morphology during the Cretaceous

Highlights

- Modern sharks were likely benthic or benthopelagic in origin
- Sharks have independently expanded to the pelagic zone several times
- Pectoral fin shape shows signatures of adaptive evolution
- Sea surface temperature impacts shark evolution

Authors

Phillip C. Sternes, Lars Schmitz,
Timothy E. Higham

Correspondence

philsternes77@gmail.com

In brief

Sternes et al. use an integrative approach to show that sharks first expanded to the pelagic zone during the Cretaceous, linked with adaptive evolution of their pectoral fin shape. The mid-Cretaceous, a time with very high sea surface temperatures, emerges as a critical phase in shark evolution.

Report

The rise of pelagic sharks and adaptive evolution of pectoral fin morphology during the Cretaceous

Phillip C. Sternes,^{1,4,*} Lars Schmitz,² and Timothy E. Higham^{1,3}

¹Department of Evolution, Ecology, and Organismal Biology, University of California, Riverside, Riverside, CA 92521, USA

²Kravis Department of Integrated Sciences, Claremont McKenna College, Claremont, CA 91711, USA

³X (formerly Twitter): @HighamLab

⁴Lead contact

*Correspondence: philsterne77@gmail.com

<https://doi.org/10.1016/j.cub.2024.05.016>

SUMMARY

The emergence and subsequent evolution of pectoral fins is a key point in vertebrate evolution, as pectoral fins are dominant control surfaces for locomotion in extant fishes.^{1–3} However, major gaps remain in our understanding of the diversity and evolution of pectoral fins among cartilaginous fishes (Chondrichthyes), a group with an evolutionary history spanning over 400 million years with current selachians (modern sharks) appearing about 200 million years ago.^{4–6} Modern sharks are a charismatic group of vertebrates often thought to be predators roaming the open ocean and coastal areas, but most extant species occupy the seafloor.⁴ Here we use an integrative approach to understand what facilitated the expansion to the pelagic realm and what morphological changes accompanied this shift. On the basis of comparative analyses in the framework of a time-calibrated molecular phylogeny,⁷ we show that modern sharks expanded to the pelagic realm no later than the Early Cretaceous (Barremian). The pattern of pectoral fin aspect ratios across selachians is congruent with adaptive evolution, and we identify an increase of the subclade disparity of aspect ratio at a time when sea surface temperatures were at their highest.⁸ The expansion to open ocean habitats likely involved extended bouts of sustained fast swimming, which led to the selection for efficient movement via higher aspect ratio pectoral fins. Swimming performance was likely enhanced in pelagic sharks during this time due to the elevated temperatures in the sea, highlighting that shark evolution has been greatly impacted by climate change.

RESULTS

Evolutionary history of selachian ecology

The majority of the 544 extant selachian species are benthic. We classified 490 extant species by their preferred occupied habitat (STAR Methods). 342 species (70%) were predominantly benthic, 84 (17%) were benthopelagic, and 64 (13%) were pelagic (STAR Methods). Most extant pelagic selachians belong to only two orders, Lamniformes and Carcharhiniformes. Stochastic character mapping supports a non-pelagic origin of selachians (Figure 1A; STAR Methods). For the root node, we found that only in 2.8% of the 1,000 iterations was a pelagic state inferred. In 46.3% and 50.9% of the iterations, a benthic or benthopelagic state was reconstructed, respectively. Therefore, we uncovered strong support for a non-pelagic origin, but it is unclear whether the origin was benthic or benthopelagic. The initial expansion to open water occurred along the branch leading to the node defining the Lamniformes, no later than the Early Cretaceous (122.6 mya, Barremian). Carcharhiniformes expanded their habitat into the pelagic zones next (98.3 to 82.4 mya, Cenomanian to early Campanian). Thus, the expansion to pelagic habitats in both Lamniformes and Carcharhiniformes, the two orders that contain most of the extant pelagic neoselachians, dates back to the Early to

early Late Cretaceous. In total, we found support for five independent expansions into the pelagic zone within selachians (STAR Methods). The other three shifts occurred later, including the small cookiecutter sharks (Squaliformes; 63.2 to 49.8 mya, early Paleogene) and, much more recently, the small spined pygmy shark (*Squaliolus laticaudus*) and the large and relatively slow whale shark (*Rhincodon typus*).

Evolution of pectoral fin aspect ratio

The distribution of pectoral fin aspect ratio across selachians is congruent with a pattern generated by adaptive evolution, as suggested by the results of evolutionary model fitting⁹ and the agnostic detection of selective regime shifts.^{10,11} We fitted several evolutionary models to the data⁹ (STAR Methods) and found very strong support for an Ornstein-Uhlenbeck (OU) model with three adaptive peaks that reflect the different habitat categories. The inferred peaks agree well with the observed group means, especially for aspect ratio. Therefore, both aspect ratio and body size show signatures of adaptive evolution, but with aspect ratio experiencing stronger selection (median estimate of α for aspect ratio is 3.77 compared to 1.92 for precaudal length [PCL]). However, there were considerable ranges of aspect ratio across all three groups as benthic selachians ranged from 1.1 to 4.3 (mean = 2.3), benthopelagic selachians ranged

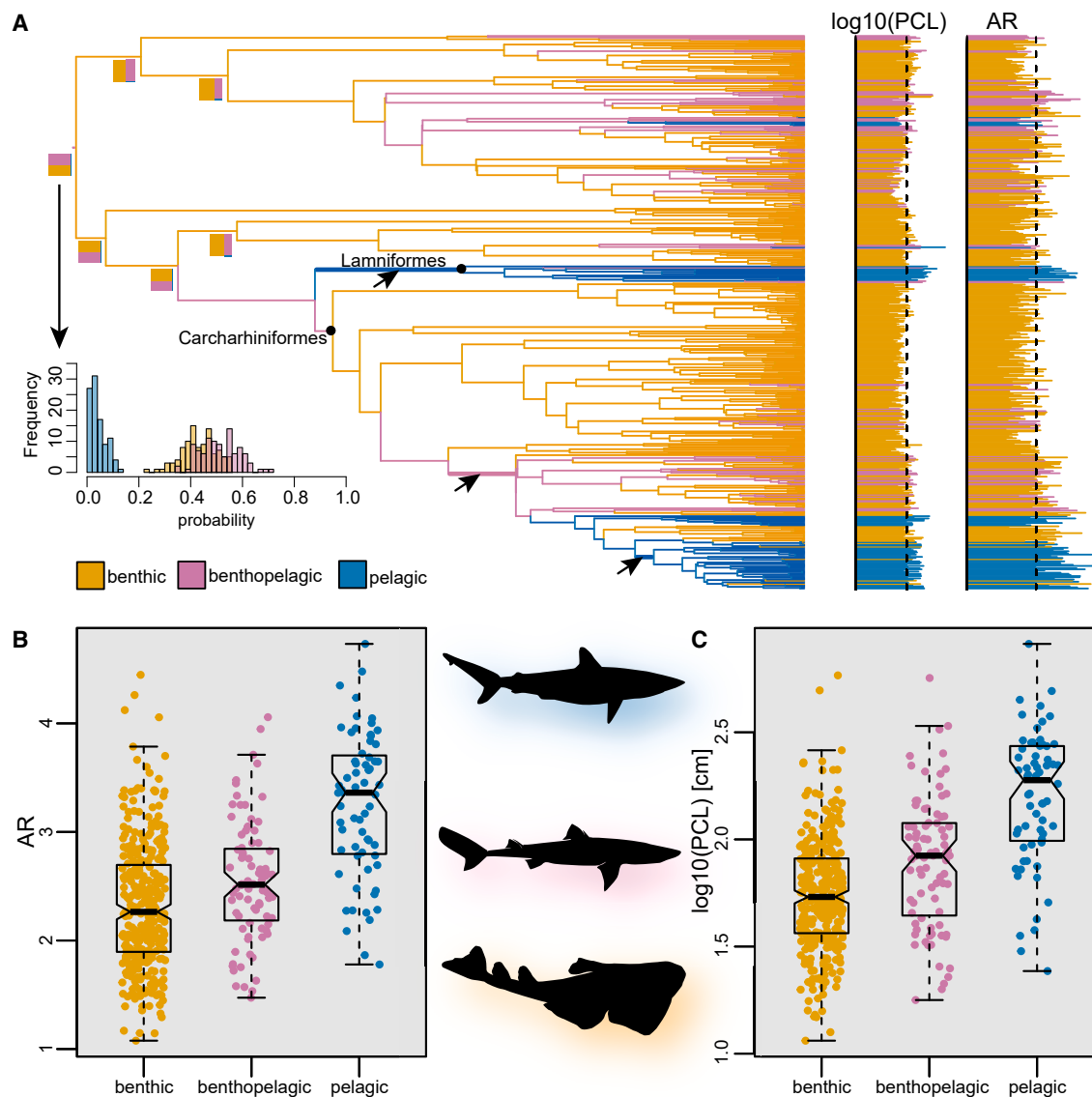


Figure 1. Ancestral state reconstructions of preferred habitat and visualization of pectoral fin aspect ratio and body size (log₁₀ of precaudal length)

(A) Maximum clade credibility tree of the selachians in this study. Branches are colored by habitat and represent results of ancestral-state reconstructions obtained from stochastic character mapping (STAR Methods). Posterior probabilities strongly suggest a non-pelagic origin of neoselachian sharks, irrespective of whether the ancestral state reconstructions are performed over the maximum clade credibility tree or over a random sample of 100 trees from the pseudo-posterior distribution (histogram). The bar plots are aligned with the phylogeny and illustrate the distribution of aspect ratio and log₁₀(PCL). Numbers signify transitions to pelagic habitats: (1) Lamniformes, (2) Carcharhiniformes 1, (3) cookiecutter sharks, (4) *Rhincodon typus* (whale shark), and (5) *Squaliolus laticaudus* (spined pygmy shark). Arrows indicate strongly supported selective regime shifts of aspect ratio. Select major lineages labeled.

(B) Boxplot of pectoral fin aspect ratio in benthic, benthopelagic, and pelagic sharks.

(C) Boxplot of log₁₀ (precaudal length) in benthic, benthopelagic, and pelagic sharks. In both boxplots, the thick line represents the median, with the box outlining the interquartile range, the difference between the first and third quantiles (IQR = Q3 – Q1). Whiskers delineate Q1 – 1.5 * IQR and Q3 + 1.5 * IQR, respectively. Silhouettes of angel, dogfish, and carcharhinid sharks were downloaded from www.phylopic.org (all downloaded images were available for reuse under the Public Domain Dedication 1.0 license).

from 1.5 to 4.1 (mean = 2.5), and pelagic selachians ranged from 1.8 to 4.7 (mean = 3.3).

At least three major selective regime shifts of aspect ratio evolution are present within selachians, mostly congruent with the lamniform and carcharhiniform transition to pelagic habitats. Using an agnostic approach^{10,11} (STAR Methods) to characterize

the adaptive landscape of aspect ratio, we found three very strongly supported shifts (Figure 1A). The oldest adaptive peak shift occurred with the origin of Lamniformes, directly coinciding with the initial shift to pelagic habitats no later than 122.6 mya (Barremian). Within Lamniformes, the adaptive peak for aspect ratio is estimated at 3.25, 1.52 times higher than the ancestral

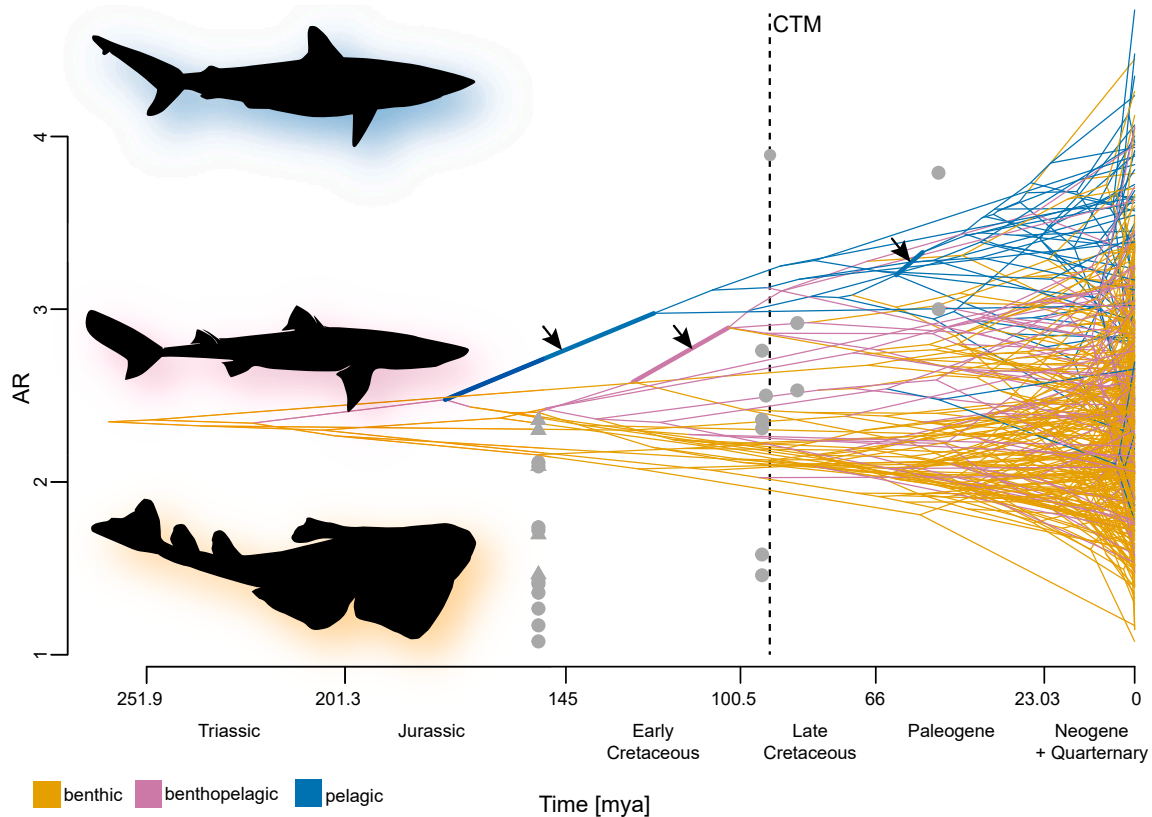


Figure 2. Traitgram projections of pectoral fin aspect ratio using a time-calibrated phylogeny

Gray shapes represent the pectoral fin aspect ratios measured in fossil specimens (supplemental information). Arrows indicate strongly supported selective regime shifts of aspect ratio. Silhouettes were downloaded from www.phylopic.org (all downloaded images were available for reuse under the Public Domain Dedication 1.0 license).

peak of 2.14. Two more selective regime shifts occurred within the Carcharhiniformes, successively increasing the adaptive peak value for aspect ratio to 2.9 (127.9 to 103.6 mya, Hauterivian to Albian) and then 3.55 (60.8 to 54 mya, Paleocene to Eocene). The regime shifts in carcharhiniforms do not precisely line up with inferred shift toward pelagic habitats in this clade, as the older shift precedes the evolution of pelagic habitats and the more recent one lags behind (Figure 1A). No additional selective regime shifts were strongly supported, indicating that the transitions to pelagic habitats in cookiecutter sharks, the spined pygmy shark, and the whale shark did not impact the evolution of pectoral fin aspect ratio. The support for selective regime shifts varies between analyses performed over a subsample of trees in the posterior distribution, but all three regime shifts identified for the consensus tree generally receive very strong support (STAR Methods). The selective regime shift in lamniforms was strongly supported in 10 out of 10 iterations; the two shifts in carcharhiniforms in 7 out of 10. Estimates of the phylogenetic half-life indicate that it took less than 200,000 years for pectoral fin aspect ratio to evolve halfway toward a new peak.

Lamniforms and carcharhiniforms evolved high pectoral fin aspect ratio in succession, which was not only suggested by the timing of the selective regime shifts but also visible in an evolutionary traitgram¹² (STAR Methods; Figure 2). The traitgram visualizes the shifts toward higher aspect ratio by plotting a

projection of the phylogenetic tree in the space defined by aspect ratio and time. In particular, the branch leading to the lamniforms (node age 122.6 mya) and the branch leading to an early node within the carcharhiniforms (node age 103.6 mya) feature noticeable increases of aspect ratio. Given that the traitgram is based on ancestral state reconstruction of only living species, we superimposed fossil data (Figure S3; STAR Methods) onto this space. Late Jurassic sharks had low aspect ratio, while Late Cretaceous sharks achieved aspect ratio in the range of modern pelagic selachians, reinforcing the view that selachians became pelagic during the Cretaceous.^{13–17}

The evolutionary traitgram and the fossil record suggest an increase in the overall disparity of the pectoral fin aspect ratio during the early Late Cretaceous, and this pattern is confirmed with a subclade-disparity-through-time analysis. Selachian subclade disparity exceeds the null expectation at 93.7 mya (early Turonian), at which time the data deviate significantly from the pattern expected under a Brownian motion (BM) model of trait evolution (STAR Methods; Figure 3B). The timing of the deviation from the BM expectation overlaps with the Cretaceous Thermal Maximum (CTM), which featured global average sea surface temperatures (SSTs) of 28.2°C.⁸ Upon exceeding the null expectation at 93.7 mya, the subclade disparity continued to rise, a trend that persisted even over the last 30 million years, which experienced a substantial cooling of SST.

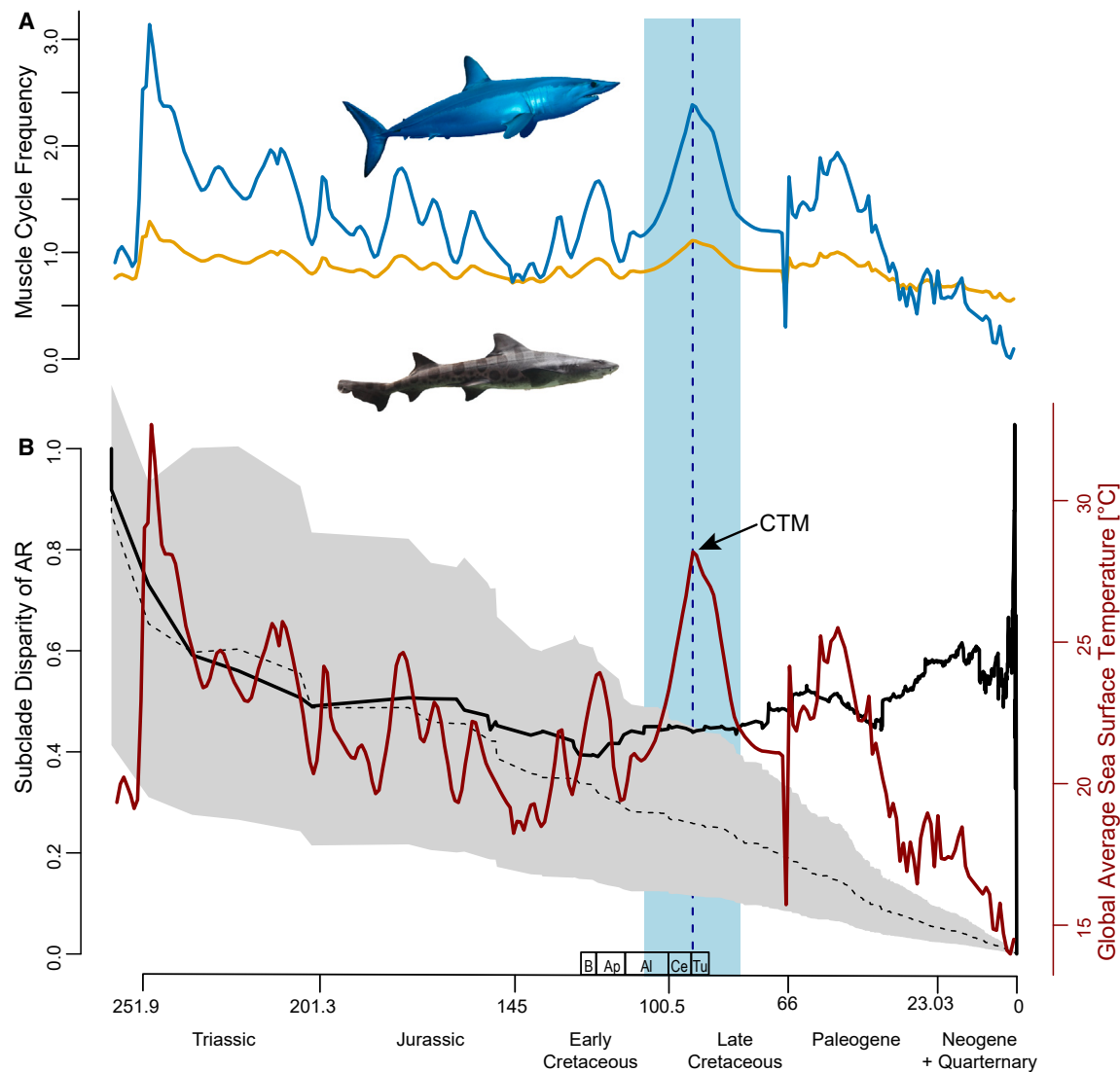


Figure 3. Selachian swimming performance and subclade disparity of aspect ratio over the past 252 million years

Muscle cycle frequency comparing benthic (orange line) and pelagic (blue line) shark species is shown in (A). Muscle cycle frequency can be considered a proxy for tailbeat frequency and therefore swim speed. Subclade disparity (solid black line) over time is shown in (B). The dashed line represents the average subclade disparity expected under a Brownian motion (BM) model of trait evolution. The gray area represents 95% confidence interval for average subclade disparity under BM. Red line shows average global sea surface temperatures (SSTs) from Scotese et al.⁸ Average subclade disparity exceeds the BM confidence interval during the early Late Cretaceous (dashed blue line). The blue region represents the phylogenetic uncertainty of when subclade disparity began to exceed the subclade disparity expected under a BM model of trait evolution (STAR Methods). Shark images were downloaded from https://commons.wikimedia.org/wiki/Main_Page (both downloaded images were available for reuse under Creative Commons Attribution-Share Alike 3.0 Unported license).

Evolution of swimming performance

Given the strong influence of temperature on muscle power output in fishes,¹⁸ we used existing data to estimate the influence of changing ocean temperatures on the power output (and therefore swimming performance) of pelagic and benthic sharks through time. Using *in vitro* muscle data from Donley et al.¹⁹ to estimate swimming performance between benthic and pelagic selachians, we found that the latter likely had much higher swim speeds compared to benthic selachians during the CTM. Muscle performance data in mako and leopard sharks across a range of temperatures suggest that power output was significantly enhanced in the pelagic mako shark with temperatures up to

28°C, whereas power output of the benthic leopard shark muscle declined slightly at the warmer temperatures¹⁹ (Table S1). Additionally, the maximum power output occurred at a higher muscle cycle frequency in the mako compared to the leopard shark.¹⁹ Muscle cycle frequency can be considered a proxy of tailbeat frequency, and therefore swim speed. Thus, mako sharks can power swim at greater sustained speeds than leopard sharks if their red muscle remains above 20°C. Estimates of benthic and pelagic selachian muscle cycle frequency (which produces peak power) over the last 250 million years demonstrate that, on average, pelagic selachians consistently have higher predicted swim speeds compared to benthic selachians (Figure 3A). Differences

in predicted swimming performance between benthic and pelagic selachians were pronounced during the early Late Cretaceous (Figure 3A).

DISCUSSION

We found that selachians were benthic or benthopelagic in origin and expanded into the pelagic zone during the Early Cretaceous (by 122.6 mya) when SSTs were substantially higher than today. In alignment with the fossil record^{13,15,16} and previous studies,^{17,20} Lamniformes were the first to expand into the pelagic zone, where they experienced an increase in net diversification rates.²¹ Carcharhiniformes were the next group to expand into the pelagic zone, where they also experienced an increase in net diversification rates.²¹ These independent expansions occurred during the Cretaceous, and Lamniformes and Carcharhiniformes to this day contain the overwhelming majority of the extant pelagic selachians.

Pectoral fins are control surfaces that play critical roles in positioning and swimming in almost all species of fishes.^{2,3,22–26} Like overall body form, pectoral fin morphology is considered to be closely related to ecology.^{22,24,25} Pectoral fin aspect ratio is routinely examined in fishes given its important role in swimming.^{2,3,22–27} For example, among labrid fishes, species with higher aspect ratio pectoral fins swim fast whereas species with lower aspect ratio pectoral fins swim relatively slowly and frequently maneuver with their pectoral fins.²⁴ For the limited shark species studied to date, there has been no clear quantitative difference in pectoral fin shape among species differing in ecology.²⁸ However, some empirical and theoretical evidence suggested that benthic selachians have short, rounded (i.e., low aspect ratio) pectoral fins, whereas pelagic selachians have long and narrow (i.e., high aspect ratio) pectoral fins.^{4,14–16,22,26–36}

We found evidence for adaptive evolution of pectoral fin aspect ratio. This suggests that habitat imposes a strong functional demand on pectoral fin morphology. For example, unlike benthic or benthopelagic selachians that can rest on the substrate, pelagic selachians are obligate ram ventilators that are constantly moving in the water column,^{29,30,34,36} which may be energetically demanding. Thus, the higher pectoral fin aspect ratio selected for in pelagic selachians may be a morphological adaptation to lower its energetic demands.^{3,4,29,30,34,36}

In addition to higher pectoral fin aspect ratio, we found pelagic selachians tended to be larger in body size (PCL) compared to benthic and benthopelagic selachians (Figure 1C). Despite their considerable body size range, the generally larger body size of pelagic selachians, which often perform long-distance migrations and occupy high levels of the marine food web, suggests that larger body size is a key morphological adaptation for the pelagic zone.^{4,36,37} While we did not find an association between aspect ratio and PCL across all sampled species, we note that larger pelagic selachians had higher pectoral fin aspect ratio compared to smaller pelagic selachians (STAR Methods; Figure S1B). Having a larger body size has several benefits including increased buoyancy, increased energy storage, the ability to travel farther, and having fewer predators.^{34,36,38,39} However, moving a larger body size in water is energetically demanding,^{26,40} suggesting that there might be increased selection for higher pectoral fin aspect ratio and increased energetic efficiency.^{3,26,27,33,34}

A critical phase in shark evolution

The Barremian to Cenomanian ages appear to be critical phases in selachian evolution.²¹ Our phylogenetic comparative analyses of extant species suggest that selachians had expanded to open-water habitat regions by the Barremian and pectoral fin aspect ratio had experienced two major increases prior to the Cenomanian (Figures 1 and 2). The benthic to benthopelagic origin and the timing of the initial expansion to the pelagic zone are congruent with the fossil record and previous phylogenetic reconstructions.^{13,15–17} Fossilized vertebral centra indicate that lamniform sharks had reached body sizes exceeding 6 m in total length by the Albian,^{41,42} a body size compatible with pelagic ocean cruisers. The Cenomanian features the evolution of the lamniform †*Cretoxyrhina mantelli*, the Cretaceous analog to the modern great white shark.⁴³ Commonly referred to as the ginsu shark, †*Cretoxyrhina mantelli* was the apex predator in a fauna that marks a global diversification event for actinopterygians and elasmobranchs.^{21,43,44} This taxonomic diversity peak coincides with high subclade disparity, which suggests that selachian lineages independently evolved similar aspect ratios (Figure 3B). Direct measurements of the aspect ratio in fossils suggest a possible mismatch between the evolutionary traitgram, which we use as a visualization but not an analytical tool, and the fossil record. In the deep parts of the tree, during the Late Jurassic, the majority of fossils have aspect ratio below the reconstructed values in the traitgram. The traitgram uses ancestral state reconstructions based on a BM process, and the computational approach based on BM favors the reconstruction of average values near the root. The maximum likelihood root estimate is similar to a “weighted average” in which the weights are determined by the topology and branch lengths of the phylogenetic tree. Given that BM is a stochastic process, one would expect traits to evolve away from the starting point at the root, roughly evenly in both directions, toward larger and smaller aspect ratio values. The low fossil aspect ratio values could potentially mean that the ancestral state reconstructions in the traitgram are inaccurate, but two points are worth discussing in this context. First, ancestral state reconstructions based on extant species alone come with wide error margins, in particular in the deep parts of a phylogenetic tree (Figures S2 and S3). While not necessarily inaccurate, it is important to keep the loose constraint of the reconstructions in the phenogram in mind. Second, bias in the fossil data toward low aspect ratio cannot be excluded. Preservation and sampling bias may partially have contributed to the predominance of low aspect ratios among Jurassic fossils. For example, many fossils in our data come from the Jurassic localities in Southern Germany (including Solnhofen), which formed in a shallow, restricted marine environment.¹⁴ The fossils from Cretaceous localities in both Lebanon and the Western Interior Seaway are from slightly deeper and less restricted marine environments^{45,46} compared to the Jurassic localities in Southern Germany. The fossils from the Cretaceous localities tended to show higher aspect ratio compared to the Jurassic localities (Figure S3). The Eocene localities in Monte Bolca are also regarded as a shallow water habitat,⁴⁷ but unlike fossils from the Jurassic in Southern Germany, fossil species with higher pectoral fin aspect ratio were present (Figure S3). While much remains to be learned about

the fossil record of selachian shark evolution, the currently available data suggest that aspect ratio >2.5 did not become common until the “mid-Cretaceous” (Figure 3).

Sea surface temperature, swimming performance, and pectoral fin evolution

Given temperature has affected shark evolution and diversity during other periods,^{21,44,48–51} it is perhaps unsurprising that we found the “mid-Cretaceous” was an important point for shark evolution as it was a period with a volatile climate such as ocean anoxic events and very warm SST.⁸ For instance, global SST averaged 23°C during the Late Cretaceous with the CTM or Cenomanian-Turonian Thermal Maximum representing the warmest temperature (28.2°C global average SST) that has occurred in the last 200 million years.⁸ Subclade disparity exceeded the BM expectation during the CTM (Figure 3), and the high SST likely had a profound effect on the swimming performance of selachians.

Among ectotherms, warmer temperatures typically lead to increases in muscle-driven performance.¹⁸ Fishes are no exception, with swim speeds increasing with rising temperature.^{18,19,40,52,53} For selachians, pelagic species can power swimming at greater sustained speeds, at temperatures above 20°C, compared to benthic species.¹⁹ While muscle performance data in sharks are limited to two species,¹⁹ such a comparison is worthwhile as this provides us with a general understanding of shark swimming performance across time. When taking these limited performance data into consideration, benthic and pelagic selachians probably swam at different speeds under the range of temperatures they experienced for the last 250 million years. We investigated the history of selachian swim speeds by incorporating previously published data on muscle performance in sharks.¹⁹ Muscle performance data in mako and leopard sharks across a range of temperatures suggest that power output was significantly enhanced in the pelagic mako shark with temperatures up to 28°C, whereas power output of the benthic leopard shark muscle declined slightly at the warmer temperatures.¹⁹ Muscle cycle frequency can be considered a proxy of tailbeat frequency, and therefore swim speed, and Donley et al.¹⁹ found that the mako exhibits peak power at higher cycle frequencies (2 versus 1 Hz) than leopard sharks if their red muscle remains above 20°C. Extending these data to the species in our study provided estimates of benthic and pelagic selachian muscle cycle frequency (that produces peak power) over the last 250 million years (STAR Methods) and demonstrate that pelagic sharks consistently have higher predicted swim speeds compared to benthic sharks (Figure 3A; STAR Methods). Differences in predicted swimming performance between benthic and pelagic selachians were pronounced during the early Late Cretaceous, a period of elevated water temperatures (Figure 3A). Extant pelagic sharks are known to frequently exploit warmer waters, including those formed anthropogenically, for thermoregulation and as a strategy to increase swimming performance.⁵⁴ Although pelagic selachians had greater sustained speeds compared to benthic selachians, that does not mean the pelagic selachians could tolerate the extremely warm tropical waters of the Late Cretaceous. For example, fossil evidence shows the lamniform shark genus †*Cardabiodon* had an antitropical distribution,⁵⁵ suggesting that the Late Cretaceous tropical waters placed a physiological limit on some species of selachians.

Limited studies suggest pelagic selachians swim faster than benthic selachians, which is likely associated with an increased cost of transport (COT),^{27,36,40,56} or the energy expended per unit body mass for a given distance traveled across varying speeds.^{27,36,40,56} A high COT could negatively affect fitness,^{56,57} so selection likely favored individuals that minimized COT via morphological changes. Increasing the lift-to-drag ratio of the pectoral fins by increasing fin aspect ratio is one mechanism.^{26,27,36} Thus, we hypothesize that an increase in global SST led to an increase in shark swim speeds due to increased muscle performance, which, in turn, facilitated the expansion into the pelagic zone. Once in this new ecological zone, individuals that had higher aspect ratio pectoral fins were likely at an evolutionary fitness advantage, leading to higher aspect ratio fins in the pelagic species.

While the increase in SST may have been a key environmental factor for both the expansion to the pelagic zone and initial increase in aspect ratio subclade disparity, SST alone cannot explain the continued increased aspect ratio subclade disparity (Figure 3B). For example, even during the cooling phase over the last 30 million years aspect ratio subclade disparity remains high (Figure 3B). This pattern suggests that other factors must be important for the evolution of pectoral fin aspect ratio. For example, the continued appearance of coral reefs and changes in prey type over time have been linked to selachian evolution and morphological specializations.^{4,17,58} This interesting paradigm warrants further research.

Our integrative study suggests temperature was one important factor in driving the evolution of selachian ecology and morphology. COT increases with swim speed, body size, and temperature, and all three of these are likely impacting the fitness of pelagic sharks at the maximum SST in the “mid-Cretaceous,” jointly driving the selection of both more streamlined bodies^{26,27,36} and high pectoral fin aspect ratio. The trifecta of swim speed, body size, and temperature and its impact on COT^{27,36,40,56} may also explain how some pelagic sharks do not see an increase in aspect ratio—maybe these sharks are not swimming as fast, or are as large, or are active in cooler waters. The absence of well-supported selective regime shifts for higher aspect ratio in the small cookiecutter sharks, the even smaller *Squaliolus laticaudus* (spined pygmy shark), and the slow-moving *Rhincodon typus* (whale shark) support such an interpretation. However, we want to clearly point out that other factors could potentially impact the evolution of pectoral fin aspect ratio. Our model fitting approach suggests that the most parameter-rich model explains the data best, and perhaps this complex model offers the only option that captures the full variability in the data. Other factors that could impact pectoral fin aspect ratio evolution might include reef habitats, which are known to impact carcharhinid diversification,¹⁷ feeding ecology,⁵⁸ regional SST differences,⁵⁹ or different locomotor physiology.^{29,30} Analyses of these factors are beyond the scope of this contribution, but we hope that future investigations will continue to explore the role of biotic and abiotic factors on shark evolution. Future studies should also expand the investigation of locomotor and habitat evolution to other groups within cartilaginous fishes, both living and extinct. For example, hybodonts, a taxonomically and ecologically diverse lineage of chondrichthyans closely related to selachians, were the dominant

chondrichthyans throughout the Triassic and Jurassic, living alongside selachians before they went extinct at the end of the Cretaceous. During the Cretaceous, hybodonts were largely restricted to freshwater habitats, interpreted as having been competitively replaced in marine habitats by selachians.¹³ Better locomotor system and modified jaw suspension have been cited for the success of selachians,^{13,60} yet details on locomotor and feeding biomechanics and their evolutionary pattern are still wanting. We posit that integrative studies that combine ecomechanical⁶¹ and ecophysiological approaches to chondrichthyan macroevolution will improve our understanding of vertebrate radiations in the oceans.

STAR★METHODS

Detailed methods are provided in the online version of this paper and include the following:

- KEY RESOURCES TABLE
- RESOURCE AVAILABILITY
 - Lead contact
 - Materials availability
 - Data and code availability
- EXPERIMENTAL MODEL AND SUBJECT DETAILS
 - Shark specimens
 - Ecological data
 - Phylogenetic data
 - Temperature data
 - Muscle performance data
- METHOD DETAILS
 - Measurements and morphological trait data
 - Habitat categorization
- QUANTIFICATION AND STATISTICAL ANALYSIS
 - Phylogenetic comparative methods
 - Estimates of swimming performance

SUPPLEMENTAL INFORMATION

Supplemental information can be found online at <https://doi.org/10.1016/j.cub.2024.05.016>.

ACKNOWLEDGMENTS

We thank P.L. Jambura for providing images of all fossil museum specimens used in this study as well as useful discussion on shark paleontology. We thank K. Shimada for useful discussion on fossil sharks and shark paleontology and a review of an earlier manuscript draft. Liam Revell helped inform our discussion of ancestral state reconstructions. We thank M. Dando and A.M. Krak for useful discussion on shark illustrations for measurements. Last, we thank the three anonymous reviewers as well as the editor for their comments and feedback that greatly improved the quality of this paper.

AUTHOR CONTRIBUTIONS

P.C.S. and T.E.H. conceptualized the study. P.C.S. collected the data. P.C.S., L.S., and T.E.H. performed research. L.S. analyzed the data. P.C.S., L.S., and T.E.H. wrote the paper.

DECLARATION OF INTERESTS

The authors declare no competing interests.

Received: February 29, 2024

Revised: April 5, 2024

Accepted: May 8, 2024

Published: June 3, 2024

REFERENCES

1. Coates, M. (2003). The evolution of paired fins. *Theory Biosci.* 122, 266–287.
2. Webb, P.W. (1982). Locomotor patterns in the evolution of Actinopterygian fishes. *Am. Zool.* 22, 329–342.
3. Fish, F.E., and Lauder, G.V. (2017). Control surfaces of aquatic vertebrates: active and passive design and function. *J. Exp. Biol.* 220, 4351–4363.
4. Compagno, L.J.V. (1990). Alternative life-history strategies of cartilaginous fishes in time and space. *Environ. Biol. Fishes* 28, 33–75.
5. Grogan, E.D., Lund, R., and Greenfest-Allen, E. (2012). The origin and early relationships of early chondrichthyans. In *Biology of Sharks and Their Relatives*, Second Edition, J.C. Carrier, J.A. Musick, and M.R. Heithaus, eds. (CRC Press), pp. 3–30.
6. Maisey, J.G. (2012). What is an ‘elasmobranch’? the impact of paleontology in understanding elasmobranch phylogeny and evolution. *J. Fish. Biol.* 80, 918–951.
7. Stein, R.W., Mull, C.G., Kuhn, T.S., Aschliman, N.C., Davidson, L.N.K., Joy, J.B., Smith, G.J., Dulvy, N.K., and Mooers, A.O. (2018). Global priorities for conserving the evolutionary history of sharks, rays and chimaeras. *Nat. Ecol. Evol.* 2, 288–298.
8. Scotese, C.R., Song, H., Mills, B.J., and van der Meer, D.G. (2021). Phanerozoic paleotemperatures: the earth’s changing climate during the last 540 million years. *Earth Sci. Rev.* 215, 103503.
9. Clavel, J., Escarguel, G., and Merceron, G. (2015). mvMORPH: an R package for fitting multivariate evolutionary models to morphometric data. *Methods Ecol. Evol.* 6, 1311–1319.
10. Uyeda, J.C., and Harmon, L.J. (2014). A novel Bayesian method for inferring and interpreting the dynamics of adaptive landscapes from phylogenetic comparative data. *Syst. Biol.* 63, 902–918.
11. Uyeda, J.C., Eastman, J., and Harmon, L. (2022). bayou: Bayesian Fitting of Ornstein-Uhlenbeck Models to Phylogenies. R package version 2.2.0 (R Foundation for Statistical Computing).
12. Revell, L.J. (2012). phytools: An R package for phylogenetic comparative biology (and other things). *Methods Ecol. Evol.* 3, 217–223.
13. Thies, D., and Reif, W.E. (1985). Phylogeny and evolutionary ecology of Mesozoic Neoselachii. *Neues Jahrb. Geol. Paläontol.* 169, 333–361.
14. Kriwet, J., and Klug, S. (2004). Late Jurassic selachians (Chondrichthyes, Elasmobranchii) from southern Germany: re-evaluation on taxonomy and diversity. *Zitteliana* 444, 67–95.
15. Vullo, R., Frey, E., Ifrim, C., González González, M.A., Stinnesbeck, E.S., and Stinnesbeck, W. (2021). Manta-like planktivorous sharks in Late Cretaceous oceans. *Science* 371, 1253–1256.
16. Vullo, R., Villalobos-Segura, E., Amadori, M., Kriwet, J., Frey, E., González González, M.A., Padilla Gutiérrez, J.M., Ifrim, C., Stinnesbeck, E.S., and Stinnesbeck, W. (2024). Exceptionally preserved fossil sharks from Mexico elucidate long-standing enigma of Cretaceous elasmobranch *Ptychodus*. *Proc. Biol. Sci.* 291, 20240262.
17. Sorenson, L., Santini, F., and Alfaro, M.E. (2014). The effect of habitat on modern shark diversification. *J. Evol. Biol.* 27, 1536–1548.
18. Syme, D.A. (2006). Functional properties of skeletal muscles. In *Fish Physiology Volume 23*, R.E. Shadwick, and G.V. Lauder, eds. (Academic Press), pp. 179–240.
19. Donley, J.M., Shadwick, R.E., Sepulveda, C.A., and Syme, D.A. (2007). Thermal dependence of contractile properties of the aerobic locomotor muscle in the leopard shark and shortfin mako shark. *J. Exp. Biol.* 210, 1194–1203.
20. Sternes, P.C., and Shimada, K. (2020). Body forms in sharks (Chondrichthyes: Elasmobranchii) and their functional, ecological, and evolutionary implications. *Zool.* 140, 125799.
21. Guinot, G., and Cavin, L. (2016). ‘Fish’ (Actinopterygii and Elasmobranchii) diversification patterns through deep time. *Biol. Rev.* 91, 950–981.

22. Blake, R.W. (2004). Fish functional design and swimming performance. *J. Fish. Biol.* 65, 1193–1222.
23. Weihs, D. (2002). Stability versus maneuverability in aquatic locomotion. *Integr. Comp. Biol.* 42, 127–134.
24. Wainwright, P.C., Bellwood, D.R., and Westneat, M.W. (2002). Ecomorphology of locomotion in labrid fishes. *Environ. Biol. Fishes* 65, 47–62.
25. Kane, E.A., and Higham, T.E. (2012). Life in the flow lane: differences in pectoral fin morphology suggest transitions in station-holding demand across species of marine sculpin. *Zool.* 115, 223–232.
26. Vogel, S. (1994). *Life in Moving Fluids: The Physical Biology of Flow*, Second Edition (Princeton University Press).
27. Alexander, R.M. (2003). *Principles of Animal Locomotion* (Princeton University Press).
28. Hoffmann, S.L., Buser, T.J., and Porter, M.E. (2020). Comparative morphology of shark pectoral fins. *J. Morph.* 281, 1501–1516.
29. Lauder, G.V., and Di Santo, V. (2016). Swimming mechanics and energetics of elasmobranch fishes. In *Physiology of Elasmobranch Fishes: Structure and Environment*, R.E. Shadwick, A.P. Farrell, and C.J. Brauner, eds. (Academic Press), pp. 219–253.
30. Maia, A.M.R., Wilga, C.A.D., and Lauder, G.V. (2012). Biomechanics of locomotion in sharks, rays, and chimaeras. In *Biology of Sharks and Their Relatives*, second edition, J.C. Carrier, J.A. Musick, and M.R. Heithaus, eds. (CRC Press), pp. 125–151.
31. Wilga, C.D., and Lauder, G.V. (2000). Three-dimensional kinematics and wake structure of the pectoral fins during locomotion in leopard sharks *Triakis semifasciata*. *J. Exp. Biol.* 203, 2261–2278.
32. Wilga, C.D., and Lauder, G.V. (2001). Functional morphology of pectoral fins in bamboo sharks, *Chiloscyllium plagiosum*: Benthic vs. pelagic station-holding. *J. Morphol.* 249, 195–209.
33. Fish, F., and Shannahan, L.D. (2000). The role of the pectoral fins in body trim of sharks. *J. Fish. Biol.* 56, 1062–1073.
34. Iosilevskii, G., and Papastamatiou, Y.P. (2016). Relations between morphology, buoyancy and energetics of requiem sharks. *R. Soc. Open Sci.* 3, 160406.
35. Pridmore, P.A. (1994). Submerged walking in the epaulette shark *Hemiscyllium ocellatum* (Hemiscyllidae) and its implications for locomotion in rhipidistian fishes and early tetrapods. *Zool.* 98, 278–297.
36. Fish, F.E. (2023). Aquatic locomotion: environmental constraints that drive convergent evolution. In *Convergent Evolution: Animal Form and Function*, V.L. Bels, and A.P. Russell, eds. (Springer), pp. 477–522.
37. Cortés, E. (1999). Standardized diet compositions and trophic levels of sharks. *ICES J. Mar. Sci.* 56, 707–717.
38. Kram, R., and Taylor, C.R. (1990). Energetics of running: a new perspective. *Nature* 346, 265–267.
39. Cohen, J.E., Pimm, S.L., Yodzis, P., and Saldaña, J. (1993). Body sizes of animal predators and animal prey in food webs. *J. Anim. Ecol.* 62, 67–78.
40. Hein, A.M., and Keirsted, K.J. (2012). The rising cost of warming waters: effects of temperature on the cost of swimming in fishes. *Biol. Lett.* 8, 266–269.
41. Shimada, K. (1997). Gigantic lamnoid shark vertebra from the Lower Cretaceous Kiowa Shale of Kansas. *J. Paleontol.* 71, 522–524.
42. Frederickson, J.A., Schaefer, S.N., and Doucette-Frederickson, J.A. (2015). A gigantic shark from the Lower Cretaceous Duck Creek Formation of Texas. *PLoS One* 10, e0127162.
43. Shimada, K. (1997). Paleoecological relationships of the Late Cretaceous lamniform shark, *Cretoxyrhina mantelli* (Agassiz). *J. Vertebr. Paleontol.* 71, 926–933.
44. Friedman, M., and Sallan, L.C. (2012). Five hundred million years of extinction and recovery: a Phanerozoic survey of the large scale diversity patterns in fishes. *Palaeontology* 55, 707–742.
45. Forey, P.L., Yi, L., Patterson, C., and Davies, C.E. (2003). Fossil fishes from the Cenomanian (upper Cretaceous) of Namoura, Lebanon. *J. Syst. Palaeontol.* 1, 227–330.
46. Everhart, M.J. (2017). *Oceans of Kansas: A Natural History of the Western Interior Seaway*, second edition (Indiana University Press).
47. Friedman, M., and Carnevale, G. (2018). The Bolca Lagerstätten: shallow marine life in the Eocene. *J. Geol. Soc. London.* 175, 569–579.
48. Guinot, G., and Condamine, F.L. (2023). Global impact and selectivity of the Cretaceous–Paleogene mass extinction among sharks, skates, and rays. *Science* 379, 802–806.
49. Brée, B., Condamine, F.L., and Guinot, G. (2022). Combining paleontological and neontological data shows a delayed diversification burst of carcharhiniform sharks likely mediated by environmental change. *Sci. Rep.* 12, 21906.
50. Condamine, F.L., Romieu, J., and Guinot, G. (2019). Climate cooling and clade competition likely drove the decline of lamniform sharks. *Proc. Natl. Acad. Sci. USA* 116, 20584–20590.
51. Villafañá, J.A., Rivadeneira, M.M., Pimiento, C., and Kriwet, J. (2023). Diversification trajectories and paleobiogeography of Neogene chondrichthyans from Europe. *Paleobiology* 49, 329–341.
52. Dickson, K.A., Donley, J.M., Sepulveda, C., and Bhoopat, L. (2002). Effects of temperature on sustained swimming performance and swimming kinematics of the chub mackerel *Scomber japonicus*. *J. Exp. Biol.* 205, 969–980.
53. Claireaux, G., Couturier, C., and Groison, A.L. (2006). Effect of temperature on maximum swimming speed and cost of transport in juvenile European sea bass (*Dicentrarchus labrax*). *J. Exp. Biol.* 209, 3420–3428.
54. Barash, A., Scheinin, A., Bigal, E., Zemah Shamir, Z., Martinez, S., Davidi, A., Fadida, Y., Pickholtz, R., and Tchernov, D. (2023). Some like it hot: investigating thermoregulatory behavior of carcharhinid sharks in a natural environment with artificially elevated temperatures. *Fishes* 8, 428.
55. Cook, T.D., Wilson, M.V.H., and Newbrey, M.G. (2010). The first record of the Late Cretaceous lamniform shark, *Cardabiodon ricki*, from North America and new empirical test for its presumed antitropical distribution. *J. Vertebr. Paleontol.* 30, 643–649.
56. Jahn, M., and Seebacher, F. (2022). Variations in cost of transport and their ecological consequences: A review. *J. Exp. Biol.* 225, jeb243646.
57. Irschick, D., and Higham, T. (2016). *Animal Athletes: An Ecological and Evolutionary Approach* (Oxford University Press).
58. Bazzi, M., Campione, N.E., Kear, B.P., Pimiento, C., and Ahlberg, P.E. (2021). Feeding ecology has shaped the evolution of modern sharks. *Curr. Biol.* 31, 5138–5148.e4.
59. O'Brien, C.L., Robinson, S.A., Pancost, R.D., Sinninghe Damsté, J.S., Schouten, S., Lunt, D.J., Alsenz, H., Bornemann, A., Bottini, C., Brassell, S.C., et al. (2017). Cretaceous sea-surface temperature evolution: constraints from TEX₈₆ and planktonic foraminiferal oxygen isotopes. *Earth Sci. Rev.* 172, 224–247.
60. Maisey, J.G., Naylor, G.J.P., and Ward, D.J. (2004). Mesozoic elasmobranchs, neoselachian phylogeny and the rise of modern elasmobranch diversity. In *Mesozoic Fishes 3—Systematics, Paleoenvironments and Biodiversity*, G. Arratia, and A. Tintori, eds. (Verlag Dr. Friedrich Pfeil), pp. 17–56.
61. Higham, T.E., Ferry, L.A., Schmitz, L., Irschick, D.J., Starke, S., Anderson, P.S.L., Bergmann, P.J., Jamniczky, H.A., Monteiro, L.R., Navon, D., et al. (2021). Linking ecomechanical models and functional traits to understand phenotypic diversity. *TREE* 36, 860–873.
62. Ebert, D.A., Fowler, S., Compagno, L., and Dando, M. (2013). *Sharks of the World: A Fully Illustrated Guide* (Wild Nature Press).
63. Ebert, D.A., Dando, M., and Fowler, S. (2021). *Sharks of the World: A Complete Guide* (Princeton University Press).
64. R Core Team (2022). R: A language and environment for statistical computing (R Foundation for Statistical Computing). <https://www.R-project.org/>.

65. Pinheiro, J., and Bates, D.; R Core Team (2022). nlme: Linear and Nonlinear Mixed Effects Models. R Package version 3.1-157. <https://CRAN.R-project.org/package=nlme>.
66. Pennell, M.W., Eastman, J.M., Slater, G.J., Brown, J.W., Uyeda, J.C., FitzJohn, R.G., Alfaro, M.E., and Harmon, L.J. (2014). geiger v2.0: an expanded suite of methods for fitting macroevolutionary models to phylogenetic trees. *Bioinform* 30, 2216–2218.
67. Sternes, P.C., and Higham, T.E. (2022). Hammer it out: shifts in habitat are associated with changes in fin and body shape in the scalloped hammerhead (*Sphyrna lewini*). *Biol. J. Linn. Soc.* 136, 201–212.
68. Bigman, J.S., Pardo, S.A., Prinzing, T.S., Dando, M., Wegner, N.C., and Dulvy, N.K. (2018). Ecological lifestyles and the scaling of shark surface gill surface area. *J. Morphol.* 279, 1716–1724.
69. VanderWright, W.J., Bigman, J.S., Elcombe, C.F., and Dulvy, N.K. (2020). Gill slits provide a window into the respiratory physiology of sharks. *Conserv. Physiol.* 8, coaa102.
70. Sternes, P.C., Wood, J.J., and Shimada, K. (2023). Body forms of extant lamniform sharks (Elasmobranchii: Lamniformes), and comments on the morphology of the extinct megatooth shark, *Otodus megalodon*, and the evolution of lamniform thermophysiology. *Hist. Biol.* 35, 139–151.
71. Siders, Z.A., Caltabellotta, F.P., Loesser, K.B., Trotta, L.B., and Baiser, B. (2023). Using pictographs to explore morphological diversity in sharks. *Ecol. Evol.* 13, e9761.
72. Iliou, A.S., VanderWright, W., Harding, L., Jacoby, D.M.P., Payne, N.L., and Dulvy, N.K. (2023). Tail shape and the swimming speed of sharks. *R. Soc. Open Sci.* 10, 231127.
73. Irschick, D.J., and Hammerschlag, N. (2015). Morphological scaling of body form in four shark species differing in ecology and life history. *Biol. J. Linn. Soc.* 114, 126–135.
74. Gayford, J.H., Whitehead, D.A., Ketchum, J.T., and Field, D.J. (2023). The selective drivers of allometry in sharks (Chondrichthyes: Elasmobranchii). *Zool. J. Linn. Soc.* 198, 257–277.
75. Gayford, J.H., Whitehead, D.A., and Jaquemet, S. (2024). Ontogenetic shifts in the body form in the bull shark (*Carcharhinus leucas*). *J. Morphol.* 285, e21673.
76. Bollback, J.P. (2006). Stochastic character mapping of discrete traits on phylogenies. *BMC Bioinform* 7, 88.
77. Grafen, A. (1989). The phylogenetic regression. *Philos. Trans. R. Soc. Lond. B Biol. Sci.* 326, 119–157.
78. Pinheiro, J.C., and Bates, D.M. (2000). *Mixed-Effects Models in S and S-Plus* (Springer).
79. Evans, M.E.K., Smith, S.A., Flynn, R.S., and Donoghue, M.J. (2009). Climate, niche evolution, and diversification of the “bird-cage” evening primroses (*Oenothera*, sections *Anogra* and *Kleinia*). *Am. Nat.* 173, 225–240.
80. Harmon, L.J., Schulte, J.A., Larson, A., and Losos, J.B. (2003). Tempo and mode of evolutionary radiation in iguanian lizards. *Science* 301, 961–964.

STAR★METHODS

KEY RESOURCES TABLE

REAGENT or RESOURCE	SOURCE	IDENTIFIER
Deposited data		
Extant selachian morphometric data	Ebert et al., ⁶² This paper	https://doi.org/10.17605/OSF.IO/FKQPU
Ecological data	Ebert et al. ⁶³	https://doi.org/10.17605/OSF.IO/FKQPU
Extinct selachian morphometric data	This paper	Figure S3, https://doi.org/10.17605/OSF.IO/FKQPU
Maximum clade credibility tree	Stein et al. ⁷	https://doi.org/10.17605/OSF.IO/FKQPU
SST Data	Scotese et al. ⁸	https://doi.org/10.17605/OSF.IO/FKQPU
Selachian <i>in vitro</i> muscle data	Donley et al. ¹⁹	Table S1
Phylogenetic Comparative Analyses	This paper	https://doi.org/10.17605/OSF.IO/FKQPU
Software and algorithms		
ImageJ	National Institutes of Health and the Laboratory for Optical and Computational Instrumentation (LOCI, University of Wisconsin)	https://imagej.net/ij/download.html
R	R Development Core Team ⁶⁴	https://www.r-project.org/
mvMorph (R Package)	Clavel et al. ⁹	1.0
Bayou (R Package)	Uyeda et al. ¹¹	2.2.0
phytools (R package)	Revell ¹²	1.0
nlme (R package)	Pinheiro et al. ⁶⁵	3.1
Geiger (R Package)	Pennell et al. ⁶⁶	2.0

RESOURCE AVAILABILITY

Lead contact

Further information and requests for resources should be directed to, and will be fulfilled by, the Lead Contact, Phillip Sternes (philsteres77@gmail.com).

Materials availability

This study did not generate new unique reagents.

Data and code availability

- The full dataset including the list of all species, habitat categorization, body size, and pectoral fin aspect ratios have been deposited at OSF and are publicly available as of the date of publication. DOI is listed in the [key resources table](#).
- All original code has been deposited at OSF and is publicly available as of the date of publication. DOI is listed in the [key resources table](#).
- Any additional information required to reanalyze the data reported in this paper is available from the [lead contact](#) upon request.

EXPERIMENTAL MODEL AND SUBJECT DETAILS

Shark specimens

The illustrations of shark species come from *Sharks of the World: A Fully Illustrated Guide* by Ebert et al.⁶² Pictures of extinct species were obtained from specimens housed in the Natural History Museum (NHMUK, London, United Kingdom) or from published literature.

Ecological data

We obtained all ecological on shark habitats from *Sharks of the World: A Complete Guide* by Ebert et al.⁶³

Phylogenetic data

We downloaded a time calibrated molecular phylogeny of sharks from <https://vertlife.org/sharktree/>.

Temperature data

We obtained all sea surface temperature (SST) data from Scotese et al.⁸

Muscle performance data

We used shark *in vitro* muscle data from Donley et al.¹⁹

METHOD DETAILS

Measurements and morphological trait data

Aspect Ratio is defined as the ratio of span to chord,^{26,27} or in the case of fish fins, fin length to area.^{24–28} We followed the methods of Hoffmann et al.²⁸ and Sternes and Higham⁶⁷ as we used ImageJ to measure the pectoral fin length (PFL) and pectoral fin area (PFA) of each selachian in our dataset (Figure S1A; STAR Methods). AR was calculated by PFL^2/PFA . In addition, we measured the precaudal length (PCL), total length (TL) as well (Figure S1A). Following the approaches in previous studies^{15,16,20,68–72} we used the illustrations of every extant selachian shark species from *Sharks of the World: A Fully Illustrated Guide* by Ebert et al.⁶² The purpose of the book is to help readers in identifying sharks and it consists of nearly 500 shark species drawn in lateral view (at a mature stage) except for the order Squatiniformes which is drawn in dorsal view. Additionally, in this specific field guide, there is a scale bar for each illustration. Both Sternes and Shimada²⁰ and Siders et al.⁷¹ have performed analyses comparing the illustrations from the book to real shark specimens to test for their accuracy and reliability. No major significant differences between the illustrations and preserved shark specimens were determined.^{20,71} As a guidebook, the pectoral fins are pointed ventrally (except Squatiniformes) to aid readers in comparing the shape of specimens to the illustrations for species identification. Therefore, the complete shape of the pectoral fin (e.g., area and fin length) are clearly drawn in a planar orientation. Since Squatiniformes are flattened sharks, they are presented in dorsal view but this still depicts the full pectoral fin shape in a planar view. Finally, we acknowledge there is possible variation for pectoral fin shape across individuals of a species but all current studies indicate this variation is minor.^{67,73–75} For fossil species, we used previously published images and museum specimens and each measurement is presented in Figure S3.

Habitat categorization

Species were coded as one of three habitat types, ‘benthic’, ‘benthopelagic’, or ‘pelagic’ based on their habitat descriptions from Ebert et al.⁶³ We coded each species as ‘benthic’ based on habitat keywords of ‘benthic,’ ‘on muddy bottom,’ ‘on sediment,’ ‘bottom on insular continental shelves.’ Species were coded as ‘benthopelagic’ based on the key terms of ‘demersal,’ ‘near bottom,’ or ‘near continental shelves.’ Species were coded as ‘pelagic’ based on the keywords of ‘pelagic,’ ‘epipelagic,’ ‘bathypelagic,’ ‘open ocean,’ or ‘oceanic’ (note: functionally, water depth is not critical for classification of pelagic).

QUANTIFICATION AND STATISTICAL ANALYSIS

Phylogenetic comparative methods

We performed phylogenetic comparative methods on the basis of a dated taxon-complete tree for chondrichthyans with a pseudoposterior distribution of 10,000 fully resolved trees.⁷ This tree was time-calibrated with treePL, informed by 10 calibration fossils and a soft bound on the root node of 422 mya. The backbone of our analysis rests on the maximum clade credibility (MCC) tree, but we accounted for phylogenetic uncertainty as indicated below. The complete R script of our analyses and output is available at <https://doi.org/10.17605/OSF.IO/FKQPU>.

We estimated the evolutionary history of preferred habitat with stochastic character mapping⁷⁶ implemented in the R⁶⁴ package “phytools”.¹² We generated 1,000 trait mappings over the MCC tree with all-different transition rates (ARD), as this transition model appeared to be best supported in initial computations (Table S1). To test the robustness of the root state estimate, we iterated the stochastic character mapping over a random sample of 1000 trees from the pseudoposterior distribution, generating 1000 trait mappings. We assessed the robustness of ancestral state estimates by comparing the proportions of inferred states.

To illustrate the phylogenetic and overall distribution of data on aspect ratio and PCL, we chose phylogenetic barplots and boxplots (Figure 1). Given that the patterns of aspect ratio and PCL are similar, we tested if aspect ratio scaled with PCL using phylogenetic generalized least-square regressions.⁷⁷ We assessed the support for different linear models, specifically, a simple, an intercept, and an interaction model for linear fits using both a Brownian motion (BM) and an Ornstein-Uhlenbeck (OU) correlation structure, implemented in the “nlme” package^{65,78} for R. The simple model does not allow for differences across habitat groups and fits a single line to all data. The intercept model fits lines for each habitat group separately, but only the intercept is free to vary, the slope is forced to be equal for each group. The interaction model, finally, lets all slopes and intercepts vary. AIC scores and corresponding Akaike weights point to the BM interaction model as the best linear fit (Figure S1C; STAR Methods). P-values of this linear model reveal that if there is a correlation between aspect ratio and PCL it is only present in pelagic neoselachians. In addition, the bivariate scatterplot of aspect ratio and PCL illustrates the high variance of aspect ratio for given PCL (Figure S1B).

We therefore passed on aspect ratio and PCL to additional phylogenetic comparative methods and did not calculate residuals of aspect ratio.²⁴

To determine the mode of aspect ratio and PCL evolution and test for presence of adaptive signals in the data, we turned to evolutionary model fitting with mvMORPH.⁹ We iterated the model fitting over a random subsample ($N = 100$) from the pseudo-posterior tree distribution and specifically compared the fit of the following models of trait evolution.

- (1) BM1, a BM model with a single rate for each trait;
- (2) BMM, a BM model that allows different rates for each trait;
- (3) EB, a model of trait evolution with initially fast rates that slow over time (early burst model);
- (4) OU, an Ornstein-Uhlenbeck model of trait evolution with one selective regime for the whole tree (single peak OU model); and
- (5) OUM, an Ornstein-Uhlenbeck model of trait evolution with multiple selective regimes for the tree, corresponding to pre-defined groups (multi-peak OU model). To test for hypotheses of evolutionary lag, i.e., with one trait trailing another, can be tested with asymmetrical alpha matrices (diagonal, upper, lower).

We determined the best fitting model via AIC scores and Akaike weights (Figures S1C and S1D). The OUM models emerged as the by far best supported models, yet there were no clear differences between the four OUM versions we tried (OUM, OUM diagonal, OUM upper, OUM lower). We therefore summarized the results of the basic OUM model (Figures S1E and S1F).

Next, we turned to an agnostic approach to characterize the adaptive landscape of aspect ratio evolution, a Bayesian implementation of the OU method.^{10,11} We performed the bayou-analysis for the MCC tree, letting two reversible jump Markov Chain Monte Carlo (MCMC) simulations run for 6,000,000 generations. We used half-cauchy distributions for α and σ^2 , a conditional Poisson distribution for the number of shifts (expected number of changes: 10, maximum number of changes: 50), and a normal distribution for θ , centered on the mean of aspect ratio with 1.5 standard deviations. We allowed one regime shift per branch, irrespective of branch length. After discarding the first 30% as burn-in, we checked whether the two independent MCMC chains had converged on similar regions in the parameter space with Gelman's R for log likelihood, σ^2 , and α (Figure S2A), and a bivariate plot of the posterior probabilities for shifts along branches against each other (Figure S2B). If convergence was reached, these posterior probabilities should fall along a line with a slope of one if convergence is reached. We considered shifts in the selective regime along a branch as well-supported if their respective posterior probabilities were far outside the main distribution of all probabilities (Figure S2C). With this approach, we conservatively identified 3 selective regime shifts, and confirmed that these branches received high support when we performed the bayOU analysis over a random subsample of 10 trees from the pseudo-posterior distribution.

We highlighted the position of these three very strongly supported selective regime shifts within an evolutionary traitgram of aspect ratio.⁷⁹ The evolutionary traitgram (Figure 2)⁷⁹ illustrates the inferred trait history, by plotting a projection of the phylogenetic tree in the space defined by aspect ratio. Unsurprisingly, the root ancestral state of aspect ratio is reconstructed near the average value of aspect ratio among extant neoselachians. The ancestral states are estimated by maximum likelihood, employing a BM model (the simplest evolutionary model), with no prior constraints on the root.

The early Late Cretaceous also emerges as an important time interval when calculating a subclade disparity through time plot⁸⁰ with the R package "geiger".⁶⁶ We obtained reproducible result when performing 10,000 simulations, and then iterated the disparity calculation over 100 random trees. The results from these 100 iterations allowed us to better understand when subclade disparity began to exceed the subclade disparity expected under a BM model of trait evolution (Figure 3B).

Estimates of swimming performance

We used the *in vitro* muscle data from Donley et al.¹⁹ to estimate the effects of historical changes in water temperature on the swimming performance of benthic and pelagic sharks. To do this, we used their data regarding the cycle frequency that resulted in maximum muscle power (PPF, or peak power frequency) over a range of temperatures in both mako sharks (*Isurus oxyrinchus*; 15°C to 28°C) and leopard sharks (*Triakis semifasciata*; 15°C to 25°C). Cycle frequency can be considered a proxy for tailbeat frequency, and tail beat frequency is correlated with swim speed. We ran linear regressions relating PPF to the temperatures used in their study, extracted the equations of the lines (Table S1), and then used the historical sea surface temperature data from Scotese et al.⁸ to estimate the PPF for each species over time. The equation for mako sharks was $PPF = 0.16(\text{temp}) - 2.24$ and the equation for leopard sharks was $PPF = 0.04(\text{temp}) + 0.02$.